FESC Phase 2 Technology Commercialization Projects

High Efficiency Black Polymer Solar Cells
(Progress Report May 2013)

PI: Dr. Franky So
External Collaborators: John Reynolds, Georgia Tech
Industry Partner: Sestar Technologies, LLC
Students: Cephas Small and Song Chen

Description: The objective of the proposed project is to synthesize broadly absorbing, black colored (PBLACK) polymers with especially high charge mobilities and to fabricate the highest performance polymer solar cells possible. Specifically, we will synthesize polymers with absorption band ranging from 400 nm to beyond 1 μm with carrier mobilities higher than 10^{-4} cm^2/Vs. Polymer-fullerene (both $PC_{60}BM$ and $PC_{70}BM$ along with more recently developed derivatives) blend morphology will be optimized using different solvent/heat treatments as well as additives to the blends. The final device will be enhanced using anode and cathode interlayers to enhance carrier extraction to the electrodes. With the ability to synthesize broadly absorbing polymers, control the donor-acceptor phase morphology and engineer the device structure, it is expected that the power conversion efficiency of polymer solar cells can reach 10% at the end of the two-year program.

Summary of Progress

Polymer bulk heterojunction solar cells based on low bandgap polymer:fullerene blends are promising for next generation low-cost photovoltaics. While these solution-processed solar cells are compatible with large-scale roll-to-roll processing, active layers used for typical laboratory-scale devices are too thin to ensure high manufacturing yields. Furthermore, due to the limited light absorption and optical interference within the thin active layer, the external quantum efficiencies (EQEs) of bulk heterojunction polymer solar cells are severely limited. In order to produce polymer solar cells with high yields, efficient solar cells with a thick active layer must be demonstrated. In this work, the performance of thick-film solar cells employing the low-bandgap polymer poly(dithienogermole-thienopyrrolodione) (PDTG-TPD) was demonstrated. Power conversion efficiencies over 8.0% were obtained for devices with an active layer thickness of 200 nm, illustrating the potential of this polymer for large-scale manufacturing. Although an average EQE > 65% was obtained for devices with active layer thicknesses > 200 nm, the cell performance could not be maintained due to a reduction in fill factor. By comparing our results for PDTG-TPD solar cells with similar P3HT-based devices, we investigated the loss mechanisms associated with the limited device performance observed for thick-film low-bandgap polymer solar cells.

1. Funds leveraged / New Partnerships Created

New collaborations						
Partner name	Title or short description of the collaboration				Funding, if applicable	
Proposals						
Title	Agency	Reference Number	PI, Co-investigators and collaborators	Funding requested	Project time frame (1 year, 2 years, etc.)	Date submitted
Dipole Engineering for polymer solar cells	DOE Basic Energy Science		Franky So (UF) John Reynolds (Georgia Tech)	$840,000	3 years	November, 2012
Grants Awarded						
Title	Agency	Reference Number	PI, Co-investigators and collaborators	Period of Performance	Funding awarded	

2013 Annual Report

High efficiency polymer solar cells with thick films and prototypical structure for printing

Based on the demonstration of high efficiency polymer solar cells based on a low bandgap donor-acceptor copolymer with alternating dithienogermole-thienopyrrolodione (DTG-TPD) repeat units last year, we further present high efficiency inverted polymer solar cell with thicker active layers that will potentially facilitate the production yield of roll-to-roll printing process. One key factor for improving the large-scale R2R processing compatibility of polymer solar cells is the active layer thickness required to ensure high manufacturing yields in PV modules. Most high efficiency laboratory-scale devices demonstrated have an active layer with a thickness of about 100 nm which is too thin for R2R processing to ensure a pinhole-free film. Obtaining high efficiency devices with active layers thicker than 200 nm is critical for commercialization. To achieve high efficiency with an active layer thickness larger than 200nm, we fabricated the device containing a bottom transparent oxide electrode, a ZnO-PVP composite layer with UV-ozone treatment, a photo-active layer composed of PDTG-TPD and fullerene, a layer of molybdenum oxide and a top electrode—silver. In addition, the efficiency loss mechanism in the thick devices was studied in depth by the measurement of field dependent external quantum efficiency spectra and photoconductivity analysis. The work is done in collaboration with Dr. John Reynolds at Georgia Institute of Technology.

Figure 1 shows the photocurrent density–voltage (J–V) characteristics and the corresponding external quantum efficiency (EQE) spectra for inverted PDTG-TPD:$PC_{71}BM$ solar cells with 105 nm, 204 nm, and 258 nm-thick active layers. Figure 1 a shows that the short-circuit current density (Jsc) increases with increasing active layer thickness due to enhanced light absorption, with the highest Jsc of 16.1 mA cm^{-2} obtained for the device with an active layer thickness of 258 nm. The integrated current density from the EQE spectra, shown in Figure 1 b, is consistent with the measured Jsc with 5% deviation. The difference in the EQE spectra is due to optical interference effects between the incident light and light reflected from the Ag back electrode. For devices with thickness $L \geq 200$ nm, the interference effects no longer affect the photocurrent density of the device and the active layer absorbs most of the incident light below 700 nm, resulting in EQEs above 70% from 400 nm to 700 nm.

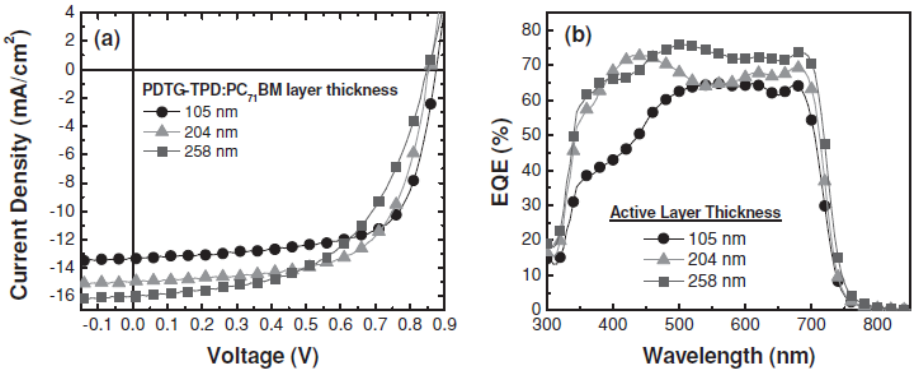

FIGURE 1 (A) CURRENT DENSITY VERSUS VOLTAGE CHARACTERISTICS FOR PDTG-TPD:PC 71 BM SOLAR CELLS WITH 105 NM, 204 NM, AND 258 NM-THICK ACTIVE LAYER. (B) CORRESPONDING EXTERNAL QUANTUM EFFICIENCY (EQE) SPECTRA FOR THE DEVICES.

Table 1 summarizes the average solar cell parameters for the PDTG-TPD:$PC_{71}BM$ devices with an active layer thickness varying from 90 nm to 409 nm. The reduction in FF observed for PDTG-TPD solar cells with increasing active layer thickness is the major factor limiting the device performance. A power conversion efficiency (PCE) of 7.9% is obtained for the device with a 105 nm thick active layer, which is consistent with our previous report.

TABLE 1 AVERAGED SOLAR CELL PERFORMANCE FOR PDTG-TPD:PC 71 BM
DEVICES WITH VARIOUS ACTIVE LAYER THICKNESS UNDER

Active Layer Thickness	J_{sc} (mA cm^{-2})	J_{sc} (EQE) (mA cm^{-2})	V_{oc} (V)	FF (%)	PCE (%)
90 nm	12.5 +/−0.1	12.3	0.88	68.5 +/−0.1	7.5 +/−0.1
105 nm	13.3 +/−0.2	13.0	0.87	68.7 +/−0.3	7.9 +/−0.1
153 nm	13.5 +/−0.4	13.5	0.86	68.1 +/− 0.3	8.0 +/−0.2
204 nm	14.9 +/−0.3	14.7	0.86	64.5 +/−0.7	8.2 +/−0.2
258 nm	16.1 +/−0.2	16.0	0.85	54.1 +/−0.9	7.4 +/−0.1
409 nm	15.2 +/−0.1	14.9	0.82	41.6 +/−0.9	5.2 +/−0.1

The efficiency remains constant for devices with $L \leq 204$ nm, with an average PCE of 8.2% being obtained for devices with an active layer thickness of 204 nm. Above 200 nm, the FF reduction becomes significant, dropping from 69% in 105 nm film to 42% in 409 nm film.

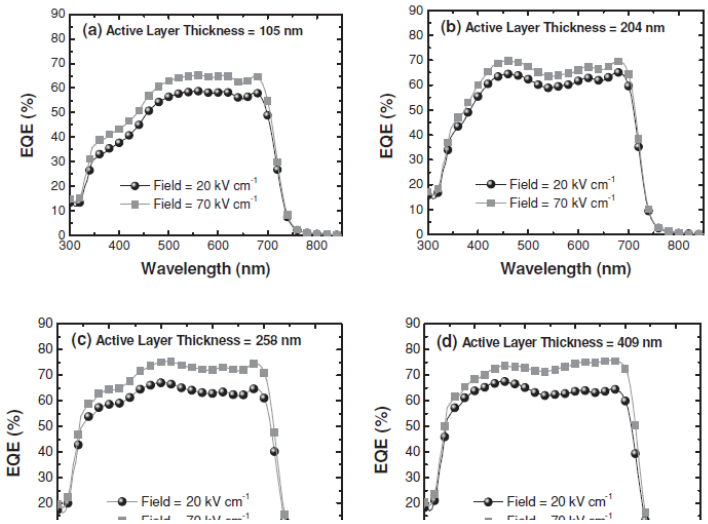

FIGURE 2 FIELD-DEPENDENT EQE SPECTRA FOR PDTG-TPD:PC 71 BM SOLAR CELLS WITH (A) 105 NM, (B) 204 NM, (C) 258 NM AND (D) 409 NM-THICK ACTIVE LAYER. THE EQE SPECTRA WERE MEASURED AT INTERNAL

To determine the root cause for the reduction in FF observed in thick-film PDTG-TPD:$PC_{71}BM$ solar cells, the EQE spectra for the thin-film and thick-film devices were measured under different values of internal electric field. **Figure 2** shows the field-dependent EQE spectra for devices with 105 nm, 204 nm, 258 nm, and 409 nm-thick active layers, respectively. By measuring the EQE as a function of internal electric field (E), approximated as $E = (Voc-V)/L$, the effect of series resistance can be eliminated. For the device with an active layer thickness ≤ 204 nm, increasing the applied fi eld from 20

kV cm^{-1} to 70 kV cm^{-1} leads to a uniform enhancement in EQE across the entire spectral range. The increased applied field enhances the extraction of photogenerated charges equally across the EQE spectrum. Interestingly, for devices with $L > 204$ nm, a stronger field dependent enhancement in EQE is observed in the spectral range from 500 to 750 nm when the applied field is increased from 20 kV cm^{-1} to 70 kV cm^{-1}. This wavelength range corresponds to the absorption spectrum for a pristine PDTG-TPD film. For devices with a thick active layer, the build-up of charges in PDTG-TPD:$PC_{71}BM$ will hinder charge collection and contribute to the FF reduction in thick solar cells.

To study the role space-charge accumulation plays in PDTGTPD: $PC_{71}BM$ solar cells with a thick active layer, we employed the SCL photocurrent model to confirm that the electrostatic space-charge limit was reached in our thick devices. We compared the results for PDTG-TPD:$PC_{71}BM$ solar cells with similar devices based on P3HT:$PC_{61}BM$, since P3HT solar cells provide a model system for studying space-charge effects. The effective photocurrent J_{ph}, normalized to the saturation photocurrent $J_{sat} = qG_{max}L$, was plotted on a double logarithmic scale against the effective voltage across the device, given by $V_{eff} = V_0 - V$. Here, V_0 is defined as the voltage where $J_{ph} = 0$ and is slightly larger than Voc. This "corrected" photocurrent analysis is a widely used tool for analyzing recombination loss processes in organic solar cells. **Figure 3a** shows the results for the PDTG-TPD:$PC_{71}BM$ solar cells with 105 nm, 258 nm and 409 nm-thick active layer. For the device with a 105 nm thick active layer, two different voltage regimes can be observed. For $V_{eff} <$ 0.30 V, J_{ph} steadily increases with voltage due to the competition between diffusion and drift for photo-generated carrier transport at low field. For $V_{eff} > 0.30$ V, the photocurrent saturates with increasing voltage. In this saturation regime, the internal field is strong enough to efficiently extract photogenerated carriers and the high field is responsible for the dissociation of *e-h* pairs. The voltage corresponding to the short circuit condition falls within the saturation regime, indicating that the high J_{sc} and FF obtained for this device is due to efficient charge collection by the internal electric field. For the device with a 105 nm active layer, space charge effects were not observed based on the data shown in Figure 3a. As the active layer thickness for PDTG-TPD cells increased above 200 nm, a square-root effective voltage dependence on J_{ph} is observed. This $J_{ph} \propto V^{1/2}$ corresponds to the onset of space-charge limited photocurrent in thick PDTG-TPD cells assuming a $J_{ph} \propto G¾$ dependence is also observed. The solid lines in Figure 3a correspond to $J_{ph} \propto V^{1/2}$. For the 409 nm-thick device, the $J_{ph} \propto V ½$ regime extends to the short circuit condition, which correlates well with the reduction in Jsc and FF observed in this device. These results are in contrast with those found in **Figure 3b** for P3HT:$PC_{61}BM$.

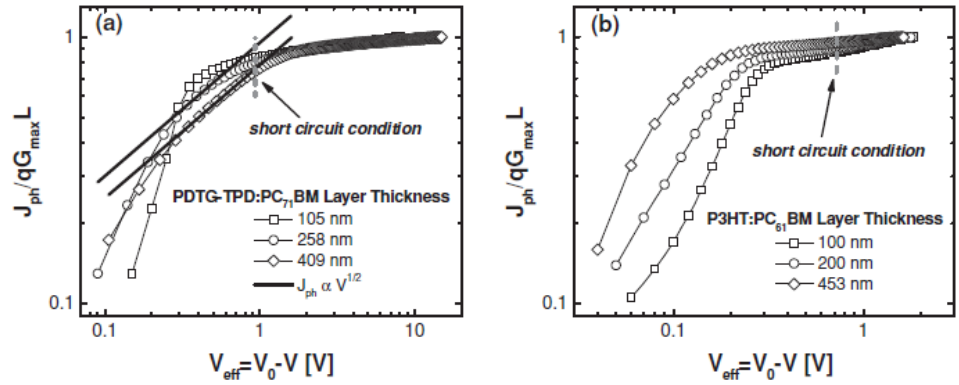

Figure 3 Effective photocurrent density (J ph) normalized by J sat = qG max L as a function of effective voltage (V_{eff}) under 100 mW cm^{-2} illumination for (a) PDTG-TPD:$PC_{71}BM$ cells with 105 nm, 258 nm, and 409 nm-thick active layer,

and (b) P3HT:PC 61 BM cells with 100 nm, 200 nm, and 453 nm-thick active layer. Dashed lines highlight the value of V_{eff} corresponding the short-circuit condition ($V_{eff} = V_0$). The solid lines correspond to $J_{ph} \propto V^{1/2}$ fits of the photocurrent in the SCL regime for PDTG-TPD solar cells.

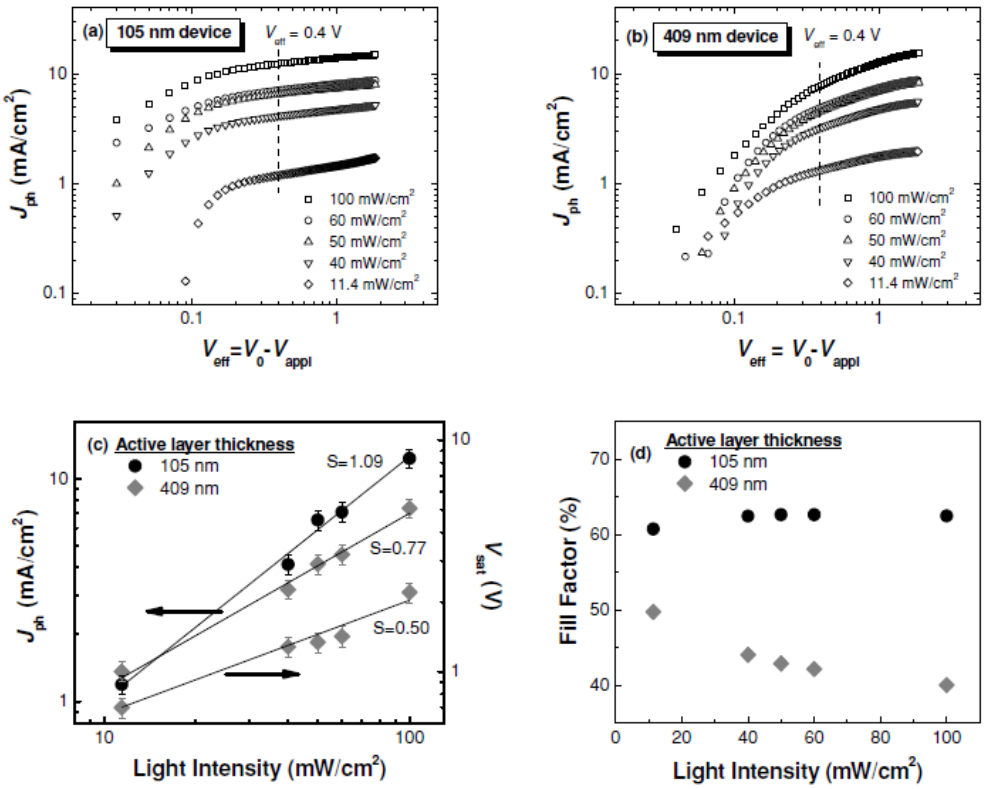

FIGURE 4 LIGHT INTENSITY DEPENDENT STUDY FOR PDTG-TPD:$PC_{71}BM$ SOLAR CELLS WITH THIN AND THICK ACTIVE LAYER. $J_{PH} - V_{EFF}$ CURVES FOR THE (A) 105 NM-THICK AND (B) 409 NM-THICK DEVICES UNDER VARIOUS LIGHT INTENSITIES (FROM 11.4 TO 100 MW CM^{-2}). (C) EFFECTIVE PHOTOCURRENT DENSITY (J PH), SATURATION VOLTAGE (VSAT), AND (D) FILL FACTOR AS A FUNCTION OF INCIDENT LIGHT INTENSITY FOR THE SAME DEVICES. THE $J_{PH} - P_0$ CURVES WERE MEASURED AT V_{EFF} = 0.4 V.

The dependence of J_{ph} and FF on incident light intensity (P_0) was plotted for the 105 nm and 409 nm-thick PDTG-TPD:$PC_{71}BM$ solar cells (see **Figure 4**). Neutral density filters were used to control the incident light intensity, which was varied from 11.4 to 100 mW cm^{-2}. The $J_{ph} - P_0$ data for the thin and thick PDTG-TPD:$PC_{71}BM$ devices, shown in Figure 4c, was extracted from the $J_{ph} - V_{eff}$ curves shown in Figures 4a and b. For the solar cell with a 105 nm-thick active layer, J_{ph} showed a linear dependence on light intensity with the slope of the linear fit tothe data equal to 1.09. In contrast, a slope of 0.77 is observed for the 409 nm-thick PDTG-TPD solar cell. The ~ 3/4 power dependence of J ph on the incident light intensity confirms the occurrence of SCL photocurrent in PDTG-TPD:$PC_{71}BM$ solar cells at low bias. The dependence of the saturation voltage (V_{sat}) on incident light intensity provides further evidence, in which a slope of 0.50 is extracted from the $V_{sat} - P_0$ data. To form a more clear physical picture, the light-intensity dependence of the FF was also analyzed and plotted in Figure 4d. The FF remained relatively constant with incident light intensity for the 105 nm-thick solar cell, which is expected since the device is not space-charge limited at P_0 = 100 mW cm^{-2} and the thickness is sufficiently thin to ensure efficient charge extraction. For the 409 nm-thick PDTG-TPD solar cell, a 24% enhancement in FF was observed as the incident light intensity was decreased from 100 mW cm^{-2} to 11.4 mW cm^{-2}. By lowering P_0 and, consequently, reducing the generation rate of charge

carriers in the thick PDTG-TPD:PC 71 BM active layer, space-charge buildup was reduced. As a result, enhanced charge carrier collection and FF was observed in the solar cell. Despite this enhancement, the FF of the 409 nm-thick device at low light intensity does not reach the value obtained in the 105 nm device. This result indicates that the reduced photocurrent observed for thick-film devices could not be completely recovered despite lowering the incident light intensity. There is still some degree of limited charge collection occurring in thick-film PDTG-TPD:$PC_{71}BM$ solar cells.

To conclude, the loss mechanism in thick-film PDTGTPD:$PC_{71}BM$ solar cells have been investigated. For polymer solar cells with an active layer thickness up to 200 nm, efficiencies in excess of 8.0% were obtained for devices under AM 1.5G illumination at 100 mW cm^{-2}. For L > 200 nm, the SCL photocurrent regime is reached, leading to limited charge collection efficiency in the devices due to space-charge accumulation. The onset of space-charge accumulation also coincides with reductions in FF and hence power conversion efficiency in thick devices. These results indicate that although high efficiencies can be obtained in solar cells with low-bandgap conjugated donor-acceptor polymers, the high density of photogenerated charge carriers could severely limit the performance of solar cells with a thick active layer.